JOURNAL OF SOLID STATE CHEMISTRY **141,** 343–351 (1998)
ARTICLE NO. SC987933

Crystal Structures and Thermal Behavior of Two New Organic Monophosphates

Leila Baouab and Amor Jouini[1]

Laboratoire de Chimie du Solide, Département de Chimie, Faculté des Sciences, Université du Centre, Monastir 5000, Tunisia

Received July 29, 1997; in revised form June 8, 1998; accepted June 23, 1998

Two new organic monophosphates, $C_3H_{12}N_2^{2+} \cdot HPO_4^{2-} \cdot H_2O$ (DAPHP) and $C_6H_{18}N_3^{2+} \cdot 2HPO_4^- \cdot 4H_2O$ (TMEDH2P), are obtained by action of H_3PO_4 with respectively 1,2-diaminopropane and *N,N,N′,N′*-tetramethylethylenediamine. DAPHP is monoclinic, $P2_1/n$, with $a = 10.653(3)$ Å, $b = 6.025(1)$ Å, $c = 13.159(2)$ Å, $\beta = 92.37(2)^\circ$, $Z = 4$, and $\rho_{measd} = 1.48$ g/cm^3. Its atomic arrangement is described by infinite polyanions, $(HPO_4)_n^{2n-}$, organized in ribbons alternating with organic cations. TMEDH2P is triclinic, with $a = 8.209(2)$ Å, $b = 8.423(2)$ Å, $c = 8.709(2)$ Å, $\alpha = 96.70(2)^\circ$, $\beta = 113.88(2)^\circ$, $\gamma = 118.02(1)^\circ$, $Z = 1$, and $\rho_{measd} = 1.39$ g/cm^3. Its structure exhibits infinite $(H_2PO_4)_n^{n-}$ chains where organic cations are anchored between adjacent polyanions. In both structures a network of strong hydrogen bonds connects the different components in the building of the crystal. © 1998 Academic Press

I. INTRODUCTION

The crystal chemistry of alkyl cations encapsulated between chains of $[HPO_4^{2-}]_n$ or $[H_2PO_4^-]_n$ polyanions is fascinating because it may lead to single crystals of polar materials. The various types of these polyanions, observed in many crystal structures, reveal the flexibility of the aggregation with respect to the chiral or achiral cations and the possible interaction of the small dipole moments of HPO_4^{2-} or $H_2PO_4^-$ units with the dipole moments of the organic moieties, which may induce acentricity in new materials. The present work continues a series of investigations into the factors influencing the dimensions of phosphoric anion–organic cation interactions. In our previous papers (1–4), the effects of base modification and protonation in this new field of compounds including organic cations and phosphoric anions, linear P_2O_7, or cyclic P_nO_{3n} ($n = 3, 4, 6$) have been mostly studied to inspect the influence of different counteranions on the conformation and hydrogen-bonding properties of organic entities and water molecules in the solid state. In this context it may be appropriate to mention that the role of counteranions is rather efficient with small acentric ones such as $(CuCl_4)^{2-}$ (5), $(HPO_4)^{2-}$ (6), or $(H_2PO_4)^-$ (7, 8). We report here the preparation and characterization of two new materials synthesized in the system org$^+$–H_3PO_4–H_2O as single crystals, where org$^+$ are 1,2-diammoniopropane $[(C_3H_{12}N_2)^{2+}]$ and *N,N,N′,N′*-tetramethylethylenediammonium $[(C_6H_{18}N_2)^{2+}]$. The two compound formulas $C_3H_{12}N_2(HPO_4) \cdot H_2O$ and $C_6H_{18}N_2(H_2PO_4)_2 \cdot 4H_2O$ are hereafter respectively denoted DAPHP and TMEDH2P.

II. CRYSTAL CHEMISTRY

1. Chemical Preparation

Crystals of DAPHP and TMEDH2P are easily prepared by slow evaporation at room temperature of an aqueous solution of H_3PO_4 and the corresponding organic molecule in the stoichiometric ratio. Schematically the reactions are:

$$H_3PO_4 + CH_3CH(NH_2)CH_2NH_2 \rightarrow [CH_3CH(NH_3)CH_2NH_3]HPO_4 \cdot H_2O$$

$$2H_3PO_4 + (CH_3)_2N(CH_2)_2N(CH_3)_2 \rightarrow [(CH_3)_2NH(CH_2)_2NH(CH_3)_2](H_2PO_4)_2 \cdot 4H_2O$$

After several weeks, the solutions lead to transparent thin single crystals of DAPHP and stout colorless monoclinic prisms of TMEDH2P. Their chemical syntheses are reproducible, and the crystals obtained in this way are pure and stable under normal conditions of temperature and humidity.

2. Crystal Data and Structure Determination

The Weissenberg and oscillation photographs taken with Cu($K\alpha_{1,2}$) radiation show that DAPHP and TMEDH2P crystallize in the triclinic and monoclinic systems. The unit cell dimensions of both salts were measured and refined using a set of high-angle reflections $14^\circ < \theta < 16^\circ$ collected

---

[1] To whom correspondence should be addressed.

0022-4596/98 $25.00

TABLE 1
Main Crystallographic Features, X-Ray Diffraction Data Collection Parameters, and Final Results for DAPHP

I. Crystal data	
Formula: $(C_3H_{12}N_2)HPO_4 \cdot H_2O$	FW = 190.14
Crystal system: Monoclinic	Space group: $P2_1/n$
$a = 10.653(3)$ Å, $b = 6.025(1)$ Å	$V = 843.9(3)$ Å^3
$c = 13.159(2)$ Å, $\beta = 92.37(2)^\circ$	$Z = 4$
$\rho_{\mathrm{calcd}}/\rho_{\mathrm{measd}} = 1.497/1.48\ \mathrm{g \cdot cm^{-3}}$	$F(000) = 408$
Linear absorption factor	$\mu(\mathrm{Mo}K\alpha) = 0.311\ \mathrm{mm^{-1}}$
Morphology	Prism
Crystal size	$0.35 \times 0.38 \times 0.25$ mm
II. Intensity measurements	
Temperature: 293 K	Wavelength: Mo$K\alpha$ (0.7107 Å)
Diffractometer: Nonius CAD4	Scan mode: $\omega/2\theta$
Monochromator: graphite plate	Scan width: $0.61 + 0.87 \tan\theta$
Variable scan speed	$T_{\max}$ per scan: 60 s
θ range:	2–25°
Background measuring time	$T_{\max}/2$
Measurement area: $\pm h, k, l$	$h_{\max} = 12$, $k_{\max} = 7$, $l_{\max} = 15$
Number of scanned reflections:	1711
Number of unique reflections:	1477 ($R_{\mathrm{int}} = 0.016$)
Reference reflection (1)	$5\bar{1}4$ (every 2 h)
Intensity decay	0.73%
III. Structure determination	
Corrections	Lorentz and polarization corrections; no absorption correction
Structure determination	SHELXS86 (9) (direct methods)
Structure refinement	SHELXL93 (10) on personal computer
Unique reflections included	1297 ($I > 2\sigma_I$)
Refined parameters[a]	161
S	1.073
Secondary extinction coefficient	0.0040(4)
R_w/R	0.088/0.029
$w = 1/[\sigma^2(F_o^2) + (0.0587P)^2 + 0.3705P]$	$P = (F_o^2 + 2F_c^2)/3$
Number of reflections per parameter	9.17
Final Fourier residual	0.283 e Å^{-3}
Largest shift/error	0.000

[a] All H-atom parameters refined; refinement on F. Atomic scattering factors from "International Tables for X-ray Crystallogrpahy" (1992, Vol. C, Tables 4, 2, 6, 8 and 6, 1, 1, 4).

TABLE 2
Main Crystallographic Features, X-Ray Diffraction Data Collection Parameters, and Final Results for TMEDH2P

I. Crystal data	
Formula: $(C_6H_{18}N_2)(H_2PO_4)_2 \cdot 4H_2O$	FW = 384.26
Crystal system: Triclinic	Space group: $P\bar{1}$
$a = 8.209(2)$ Å, $b = 8.423(2)$ Å	$V = 4496(1)$ Å^3
$c = 8.709(2)$ Å, $\alpha = 92.70(2)^\circ$	$Z = 1$
$\beta = 113.88(2)^\circ$, $\gamma = 118.02(1)^\circ$	$F(000) = 206$
$\rho_{\mathrm{calcd}} = 1.422$, $\rho_{\mathrm{measd}} = 1.39\ \mathrm{g \cdot cm^{-3}}$	
Linear absorption factor	$\mu(\mathrm{Mo}K\alpha) = 0.288\mathrm{mm^{-1}}$
Morphology	Elongated triclinc prism
Crystal size	$0.12 \times 0.13 \times 0.21$ mm
II. Intensity measurements	
Temperature: 293 K	Wavelength: Mo$K\alpha$ (0.710 Å)
Diffractometer: Nonius CAD4	Scan mode: $\omega/2\theta$
Monochromator: graphite plate	Scan width: $0.65 + 0.82 \tan\theta$
Variable scan speed	$T_{\max}$ per scan: 60 s
θ range	3–25°
Background measuring time	$T_{\max}/2$
Measurement area: $\pm h$, $\pm k$, l	$h_{\max} = 8$, $k_{\max} = 9$, $l_{\max} = 16$
Number of unique reflections:	1701
Reference reflection (1)	122 (every 2 h)
Decay	2.1%
III. Structure determination	
Corrections	Lorentz and polarization corrections; no absorption correction
Program used	SPD (11)
Computer	Micro-VAX 2000
Structure determination	MULTAN (12)
Unique reflections included	1308 ($I > 3\sigma_I$)
Refined parameters[a]	161
Esd	0.615
Weigting scheme	Unitary
Secondary extinction	$X = 5.89 \times 10^{-6}$
Number of reflections per parameter	10.56
Final Fourier residual	0.37 e·Å^{-3}
R_w/R	0.049/0.045
Largest shift/error	0.008

[a] Atomic scattering factors from "International Tables for X-ray Crystallography" (13).

with an Enraf-Nonius CAD4 diffractometer. The structural determinations show that the proper space groups are $P2_1/n$ and $P\bar{1}$ respectively for DAPHP and TMEDH2P. The average density values, measured at room temperature with toluene as the pycnometric liquid, are in agreement with the calculated densities; formula units in the cells of both crystals are deduced from these values. The chemical crystal data, the parameters used for X-ray diffraction data collection, and the strategy used for the crystal structure determinations and their results are listed in Tables 1 and 2.

3. *Thermal Behavior*

Setaram TG-DTA92 and DSC92 thermoanalyzers were used to perform thermal treatment on samples of DAPHP and TMEDH2P. The TG–DTA experiments were carried out with 7.49- and 18.72-mg samples in an open alumina crucible. The DSC analyses were carried out using weighed 9-mg samples sealed in an aluminum DSC crucible. In both techniques, samples were heated in air at heating rates of 3–5°C/min from room temperature to 400°C; an empty crucible was used as reference.

III. STRUCTURE DESCRIPTION

A large number of monophosphates of mineral or organic cations are presently well known. Their preparations involve the neutralization of H_3PO_4 with mineral carbonates or amines in water as solvent. Similarly, the atomic arrangements usually exhibit acidic monophosphate anions,

HPO_4^{2-} or $H_2PO_4^-$, organized in infinite chains, ribbons, or layers. The solvent molecules play an important role in the building of the anionic organization by forming polyanions of formulas $[HPO_4 \cdot H_2O]_n^{2n-}$ or $[H_2PO_4 \cdot H_2O]_n^{n-}$. Mineral or organic cations via respectively their polyhedral surrounding or their H bonds originating from the amine donor groups, interconnect these anionic aggregations. We describe herein the crystal structures of both DAPHP and TMEDH2P. The acidic anion of the DAPHP arranged in ribbons is found to include one molecule of solvent, whereas that of the TMEDH2P, organized in chains, uses the solvent to assemble chains.

1. DAPHP Structure Description

The final atomic coordinates and the *U* equivalent temperature factors (isotropic for H atoms) are given in Table 3. Figure 1 displays the anionic structure located at $z = \frac{1}{4}$ and viewed along the **c** direction. The polyanion resulting from the aggregation of HPO_4^{2-} and H_2O through strong hydrogen bonds forms infinite inorganic ribbons of formula $[HPO_4H_2O]_n^{2n-}$ parallel to the **b** axis. Organic cations, as shown in Fig. 2 giving the atomic arrangement, are anchored onto the anionic ribbons through hydrogen contacts. The detailed geometry of HPO_4^{2-} (Table 4) shows that the P–O bonds are significantly shorter [1.512(1)–1.528(1) Å]

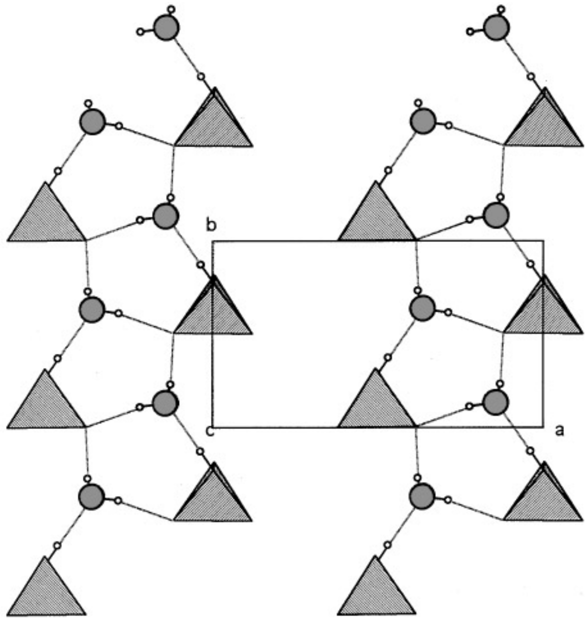

FIG. 1. Projection along the **c** direction of the $[HPO_4]H_2O$ ribbon in DAPHP. The PO_4 groups are given with a polyhedral representation. Large circles represent oxygen water molecules, and small circles indicate hydrogen atoms. Hydrogen bonds are denoted by full and dotted lines.

TABLE 3
Final Atomic Coordination and U_{eq} (U_{iso} for H Atoms) of DAPHP

Atom	$x(\sigma)$	$y(\sigma)$	$z(\sigma)$	U_{eq}(Å^2)
P	0.4988(1)	0.1435(1)	0.2986(1)	0.0183(2)
O(1)	0.4974(1)	0.2730(3)	0.1935(1)	0.0327(4)
O(2)	0.3811(1)	0.0030(2)	0.2918(1)	0.0293(3)
O(3)	0.6180(1)	0.0057(2)	0.3085(1)	0.0317(4)
O(4)	0.4948(1)	0.3178(2)	0.3828(1)	0.0279(3)
O(W)	0.6392(1)	0.6320(3)	0.1866(1)	0.0380(4)
N(1)	0.2099(2)	0.1162(3)	0.1388(1)	0.0249(4)
N(2)	0.1482(1)	– 0.1623(3)	– 0.0516(1)	0.0245(4)
C(1)	0.2620(2)	0.1408(3)	0.0363(1)	0.0266(4)
C(2)	0.2759(2)	– 0.0769(3)	– 0.0199(1)	0.0249(4)
C(3)	0.3494(2)	– 0.2523(3)	0.0391(2)	0.0341(5)
H(O1)	0.535(2)	0.382(5)	0.197(2)	0.039(7)*
H(1W)	0.628(3)	0.738(5)	0.216(2)	0.055(9)*
H(2W)	0.720(3)	0.609(5)	0.193(2)	0.057(8)*
H(1N1)	0.268(2)	0.075(4)	0.183(2)	0.036(6)*
H(2N1)	0.147(2)	0.028(4)	0.136(2)	0.031(6)*
H(3N1)	0.176(2)	0.253(4)	0.160(2)	0.040(6)*
H(1N2)	0.101(2)	– 0.194(4)	0.005(2)	0.048(7)*
H(2N2)	0.106(2)	– 0.057(4)	– 0.082(2)	0.031(5)*
H(3N2)	0.149(2)	– 0.280(5)	– 0.092(2)	0.048(7)*
H(1C1)	0.345(2)	0.205(4)	0.048(1)	0.030(5)*
H(2C1)	0.211(2)	0.238(4)	– 0.001(1)	0.031(5)*
H(C2)	0.314(2)	– 0.041(3)	– 0.080(1)	0.019(4)*
H(1C3)	0.302(2)	– 0.299(4)	0.094(2)	0.053(7)*
H(2C3)	0.428(2)	– 0.195(4)	0.065(2)	0.051(7)*
H(3C3)	0.363(3)	– 0.381(5)	0.001(2)	0.063(8)*

Note. Starred atoms were refined isotropically. Esds are given in parentheses. $U_{eq} = \frac{1}{3}\sum_i \sum_j U_{ij} a_i^* a_j^* a_i a_j$.

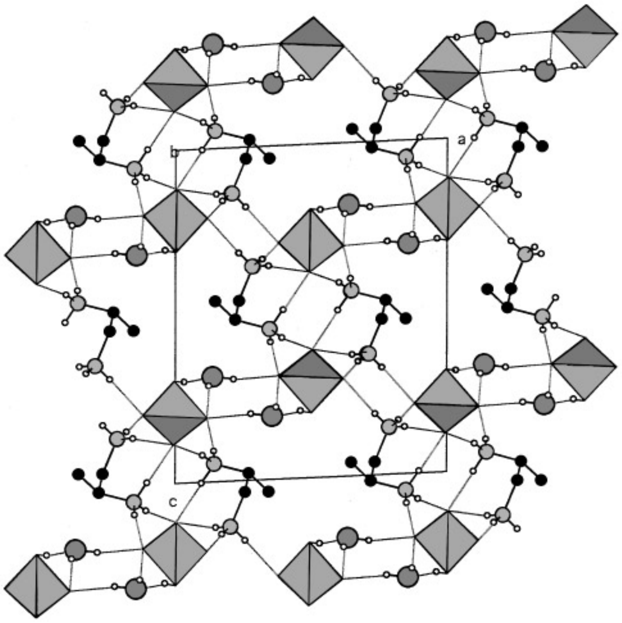

FIG. 2. Projection along the **b** direction of the DAPHP atomic arrangement. In this figure and Figs. 3 and 4, the circles represent oxygen water molecules (large dark-gray circles), nitrogen atoms (large light-gray circles), carbon atoms (small black circles), and hydrogen atoms (small white circles). Hydrogen bonds are denoted by full and dotted lines.

TABLE 4
Main Interatomic Distances (Å) and Bond Angles (Deg) in DAPHP

P	O(1)	O(2)	O(3)	O(4)
		PO_4 tetrahedron		
O(1)	1.587(1)	104.25(7)	108.76(8)	107.11(8)
O(2)	2.447(2)	1.512(1)	112.78(8)	112.29(7)
O(3)	2.525(2)	2.524(2)	1.518(1)	111.20(7)
O(4)	2.507(2)	2.525(2)	2.514(2)	1.528(1)
	P–P = 5.575(1)	P–O(1)–H(O1) = 113(2)		
		1,2-Diammoniopropane cation		
N(1)–H(1N1)	0.86(2)	H(1N1)–N(1)–H(2N1)	113(2)	
N(1)–H(2N1)	0.86(2)	H(1N1)–N(1)–H(3N1)	109(2)	
N(1)–H(3N1)	0.95(3)	H(2N1)–N(1)–H(3N1)	104(2)	
N(2)–H(1N2)	0.94(3)	H(1N2)–N(2)–H(2N2)	103(2)	
N(2)–H(2N2)	0.87(3)	H(1N2)–N(2)–H(3N2)	109(2)	
N(2)–H(3N2)	0.88(3)	H(2N2)–N(2)–H(3N2)	109(2)	
N(1)–C(1)	1.487(2)	N(1)–C(1)–C(2)	113.8(1)	
C(1)–C(2)	1.516(3)	N(2)–C(2)–C(1)	109.1(1)	
C(2)–N(2)	1.497(2)	N(2)–C(2)–C(3)	110.4(1)	
C(2)–C(3)	1.511(3)	C(3)–C(2)–C(1)	114.4(2)	

Note. Esds are given in parentheses.

than the P–OH bond [1.587(1) Å]. The H ⋯ O bonds, which maintain the cohesion of the ribbons, are characterized by relatively short distances, from 1.83(3) to 2.03(3) Å. Since the O ⋯ O distances in this hydrogen scheme [2.642(2)–2.779(2) Å] are of the same order of magnitude as in the HPO_4 acidic tetrahedron [2.447(2)–2.525(2) Å], the $[HPO_4H_2O]_n^{2n-}$ ribbons should be considered as a polyanion. The short P–P distance observed in the ribbon is 5.575(1) Å.

With regard to the organic arrangement, the main features of which are reported in Table 4, each cation is anchored onto both adjacent anionic ribbons by N–H ⋯ O hydrogen bonds. This interaction contributes to the cohesion of the structure. All the *D* (donor)–H ⋯ *A* (acceptor) hydrogen bonds are listed in Table 5 with an upper limit of 2.03(3) Å for the H ⋯ *A* distances and a lower limit of 166(2)° for the D–H ⋯ *A* bond angles (4, 14–18). Thus, this atomic arrangement exhibits three types of hydrogen bonds: (i) O(W)–H ⋯ O, including two relatively short contacts with H ⋯ O of 1.83(3) and 2.03(3) Å, (ii) O(P)–H ⋯ O, involving one short contact with H ⋯ O of 1.88(3) Å, and (iii) N–H ⋯ O, including six short distances with H ⋯ O values in the range 1.75(3)–1.98(2) Å. The first two types ensure the cohesion between PO_4 tetrahedra to build the ribbons, and the last one links parallel ribbons.

TABLE 5
Bond Lengths (Å) and Angles (Deg) in the Hydrogen-Bonding Scheme of DAPHP

	N(O)–H	H ⋯ O	N(O) ⋯ O	N(O)–H ⋯ O
N(1)–H(1N1) ⋯ O(2)	0.86(2)	1.89(2)	2.747(2)	173(2)
N(1)–H(2N1) ⋯ O(4)	0.86(2)	1.98(2)	2.831(2)	175(2)
N(1)–H(3N1) ⋯ O(2)	0.95(3)	1.75(3)	2.698(2)	176(2)
N(2)–H(1N2) ⋯ O(4)	0.94(3)	1.83(3)	2.748(2)	166(2)
N(2)–H(2N2) ⋯ O(4)	0.87(3)	1.90(3)	2.759(2)	166(2)
N(2)–H(3N2) ⋯ O(3)	0.88(3)	1.91(3)	2.779(2)	168(2)
O(W)–H(1W) ⋯ O(3)	0.76(3)	2.03(3)	2.779(2)	172(3)
O(W)–H(2W) ⋯ O(3)	0.88(3)	1.83(3)	2.695(2)	168(3)
O(1)–H(O1) ⋯ O(W)	0.77(3)	1.88(3)	2.642(2)	171(3)

Note. Esds are given in parenthesis.

2. *TMEDH2P Structure Description*

Table 6 presents the atomic coordinates and the *U* equivalent temperature factors (isotropic for H atoms). The structure can be described as being built up by chains of $H_2PO_4^-$ anions spreading with planes $y = (2n + 1)/2$ or $z = (2n + 1)/2$ and alternating with planes $y = 0$ or $z = 0$ containing the organic groups with water molecules. In the two configurations, the chains are parallel to the **a** direction. Figure 3 gives a projection in the (**b, c**) plane showing columns of anions and cations running along the **a** axis.

TABLE 6
Final Atomic Co-ordination of U_{eq} (U_{iso} for H Atoms) of TMEDH2P

Atom	$x(\sigma)$	$y(\sigma)$	$z(\sigma)$	U_{eq}(Å^2)
P	0.2063(1)	0.4320(1)	0.4821(1)	0.0256(2)
O(1)	0.1174(3)	0.5229(3)	0.3540(3)	0.0461(6)
O(2)	0.4317(3)	0.6026(4)	0.6476(4)	0.0513(8)
O(3)	0.7681(3)	0.7005(3)	0.6237(3)	0.0334(6)
O(4)	0.9372(3)	0.6616(3)	0.4462(3)	0.0388(6)
O(W1)	0.0494(3)	0.8226(4)	0.0045(5)	0.0438(7)
OW2)	0.0610(3)	0.1066(3)	0.7501(3)	0.0399(7)
N	0.3993(4)	0.8167(4)	0.1035(4)	0.0316(7)
C(1)	0.5277(6)	0.9239(6)	0.3017(6)	0.053(1)
C(2)	0.6424(6)	0.3800(5)	0.9369(6)	0.049(1)
C(3)	0.5063(5)	0.0924(5)	0.0033(5)	0.047(1)
H(O1)	0.932(5)	0.428(5)	0.616(5)	0.02(1)*
H(O2)	0.540(6)	0.641(5)	0.633(6)	0.04(1)*
H(N)	0.286(4)	0.809(4)	0.075(4)	0.01(1)*
H(1W1)	0.021(5)	0.843(4)	0.063(5)	0.01(1)*
H(2W1)	0.046(5)	0.215(5)	0.100(5)	0.04(1)*
H(1W2)	0.945(5)	0.820(5)	0.322(5)	0.03(1)*
H(2W2)	0.028(5)	0.000(5)	0.307(5)	0.02(1)*
H(1C1)	0.543(5)	0.159(5)	0.638(5)	0.02(1)*
H(2C1)	0.330(7)	0.058(7)	0.646(7)	0.07(2)*
H(3C1)	0.474(6)	0.976(6)	0.676(6)	0.04(1)*
H(1C2)	0.730(6)	0.453(6)	0.064(6)	0.05(1)*
H(2C2)	0.504(5)	0.363(5)	0.886(5)	0.03(1)*
H(3C2)	0.279(6)	0.559(6)	0.118(7)	0.06(1)*
H(1C3)	0.348(5)	0.062(5)	0.946(5)	0.03(1)*
H(2C3)	0.586(6)	0.094(5)	0.133(6)	0.05(1)*

Note. Starred atoms were refined isotropically. Esds are given parentheses. $U_{eq} = \frac{1}{3}\sum_i \sum_j U_{ij} a_i^* a_j^* a_i a_j$.

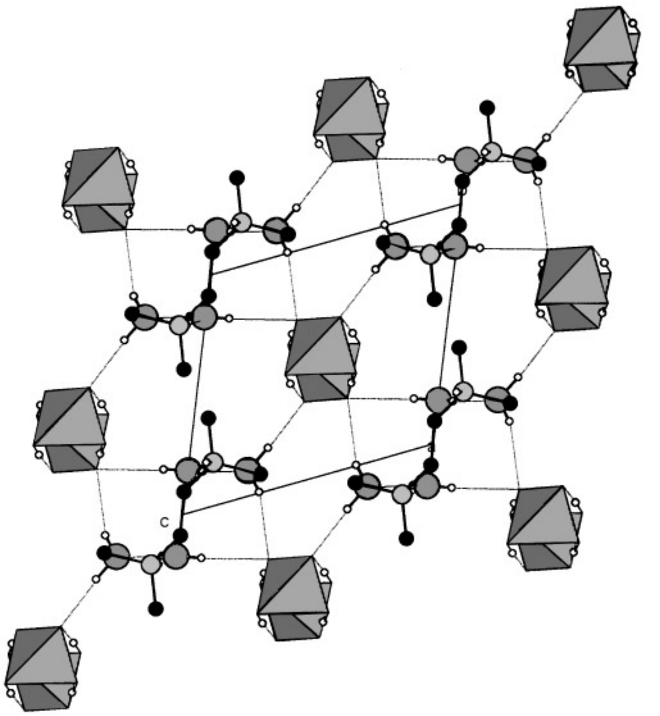

FIG. 3. Projection along the **a** direction of the TMEDH2P atomic arrangement showing the H_2PO_4 columns linked by H bonds from water molecules and organic cations. Hydrogen bonds are denoted by full and dotted lines.

Displayed in the (**a**, **c**) plane, as shown in Fig. 4, the H_2PO_4 groups, running in a parallel direction with the **a** axis, are connected by strong hydrogen bonds since the $H \cdots O$ contacts maintaining the cohesion in the chain have short distances, 1.73(5) and 1.77(5) Å. It is worth noting that the $O \cdots O$ distances involved in the hydrogen bonds [2.561(5) and 2.590(4) Å] are of the same order of magnitude as the $O \cdots O$ distances in the H_2PO_4 tetrahedron [2.455(3)–2.512(4) Å]. This and the short $P \cdots P$ distance of 4.416(1) Å allow us to consider the $[H_2PO_4]_n^{n-}$ subnetwork as a polyanion. The detailed geometry of the $H_2PO_4^-$ anion is given in Table 7. Water molecules located in planes as the organic cations are assembled in pairs linked to N atoms via O(W1) by strong hydrogen bonds, that is, O(W1)–H(1W1) $\cdots$ O(W2) [$H \cdots O$, 2.07(5) Å; $O \cdots O$, 2.742(5) Å] on one side, and N–H $\cdots$ O(W1) [$H \cdots O$, 1.85(4) Å; $N \cdots O$, 2.670(4) Å] on the other side. All the other H atoms of the water molecules are involved in H bonds with the nonprotonated oxygen atoms of adjacent $[H_2PO_4]_n^{n-}$ polyanions. As observed in the DAPHP structure, the P–O bonds, shorter than the P–OH bonds, are in accordance with data relative to the protonated oxoanions (19). The geometrical features of the organic cation, given in Table 7, are similar to those observed in the organic diphosphate $C_6H_{18}N_2 \cdot H_2P_2O_7 \cdot 2H_2O$ (20) containing the same organic molecule.

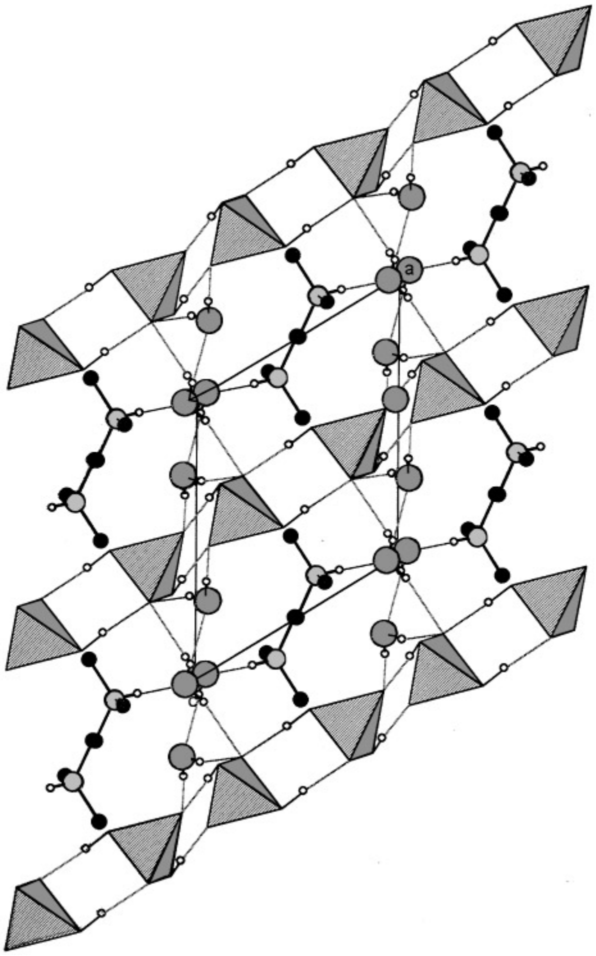

FIG. 4. Projection along the **b** direction of the TMEDH2P atomic arrangement giving the $(H_2PO_4)_n$ chains located at $y = (2n + 1)/2$ planes. Hydrogen bonds are denoted by full and dotted lines.

In this compound, atoms of tetramethylethylenediammonium were found in general positions, whereas those in the TMEDH2P are located around the $(\frac{1}{2}00)$ inversion center of the triclinic cell. The N–C and C–C distances and the C–N–C and C–C–N angles are similar and lie within the ranges 1.475(5)–1.503(6) Å and 106.8(4)–117.1(2)°, respectively. The main geometric features of the hydrogen-bonding scheme are described in Table 8. This structure includes seven potential hydrogen bond donors (one N–H and six O–H) and four O or OH acceptors. Among the acceptor atoms, O(W1) and O(W2) are single acceptors, whereas O(3) and O(4) atoms are respectively threefold and twofold acceptors.

IV. THERMAL BEHAVIOR

Thermal decomposition of DAPHP occurs in four stages between 100 and 400°C, corresponding to the successive losses of water and ammonia molecules (Fig. 5). The first

TABLE 7
Main Interatomic Distances (Å) and Bond Angles (Deg) in TMEDH2P

P	O(1)	O(2)	O(3)	O(4)
PO$_4$ tetrahedron				
O(1)	1.557(3)	107.1(2)	106.8(2)	109.8(2)
O(2)	2.505(3)	1.558(2)	110.1(2)	107.0(2)
O(3)	2.460(4)	2.512(4)	1.507(3)	115.8(2)
O(4)	2.498(4)	2.455(3)	2.543(4)	1.495(3)
P–P = 4.416(1) P–O(1)–H(O1) = 116(3) P–O(2)–H(O2) = 115(2)				
N,*N*,*N*′,*N*′-tetramethylenediammonium cation				
N–C(1)	1.475(5)		C(1)–N–C(2)	109.7(3)
N–C(2)	1.488(6)		C(1)–N–C(3)	117.1(2)
N–C(3)	1.496(6)		C(2)–N–C(3)	106.8(4)
C(3)–C(3)	1.503(6)		N–C(3)–C(3)	110.7(4)

Note. Esds are given in parentheses.

TABLE 8
Bond Lengths (Å) and Angles (Deg) in the Hydrogen-Bonding Scheme of TMEDH2P

	(N,O)–H	H ··· O	(N,O) ··· O	(N,O)–H ··· O
N(1)–H(N) ··· O(W1)	0.83(4)	1.85(4)	2.670(2)	172(4)
O(W1)–H(1W1) ··· O(W2)	0.67(5)	2.07(5)	2.742(5)	176(5)
O(W1)–H(2W1) ··· O(3)	0.81(4)	2.06(4)	2.857(3)	167(5)
O(W2)–H(1W2) ··· O(4)	0.93(5)	1.81(4)	2.735(4)	176(3)
O(W2)–H(2W2) ··· O(3)	0.76(3)	2.10(3)	2.817(3)	160(4)
O(2)–H(O2) ··· O(3)	0.86(5)	1.73(5)	2.590(4)	172(5)
O(1)–H(O1) ··· O(4)	0.79(5)	1.77(5)	2.498(4)	175(3)

Note. Esds are given in parentheses.

process starts at 100°C and is complete at 202°C. It corresponds to the loss of the only water molecule of the formula (weight loss, calculated 9.47%, experimental 9.29%), leading to a white microcrystalline powder. The second stage, from 202 to 250°C, is attributed to the further beginning of degradation and melting of the compound. Indeed, an additional treatment in a separate carbolite furnace, with a run heating of 5°C/min, leads to a very viscous yellow liquid which does not crystallize when cooled at room temperature. Apparently, the sample is polymerized and an amorphous phase, as confirmed by XRD, is formed. The TG curve shows, after the elimination of H_2O, a rather vigorous and continuous weight loss corresponding to the evolution of ammonia from the structure, probably in many steps. The DTA curve exhibits large endotherms at 142, 221, 229, and 329°C and a set of endotherms from 365 to 400°C in accordance with the elimination of the water and ammonia molecules. It should be noted that the thermal decomposition ends up in a bad smell, escaping from the resulting black product.

Figure 6 showing the DSC thermogram registered from room temperature to 250°C, reveals the same thermal behavior as DAPHP, in accordance with what is observed in

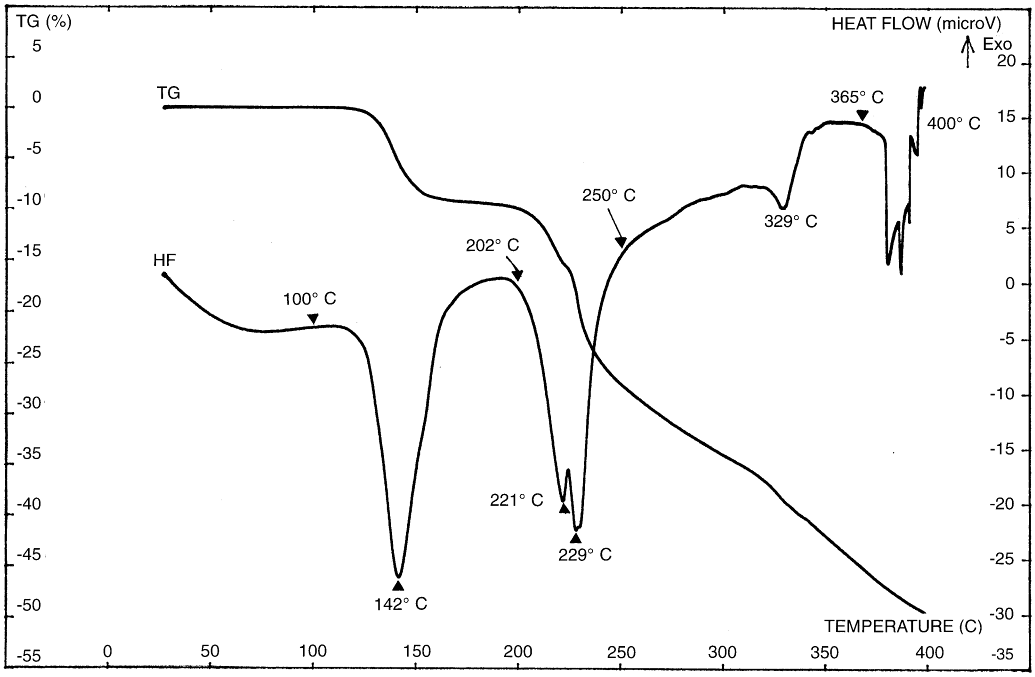

FIG. 5. TG–DTA analysis of DAPHP.

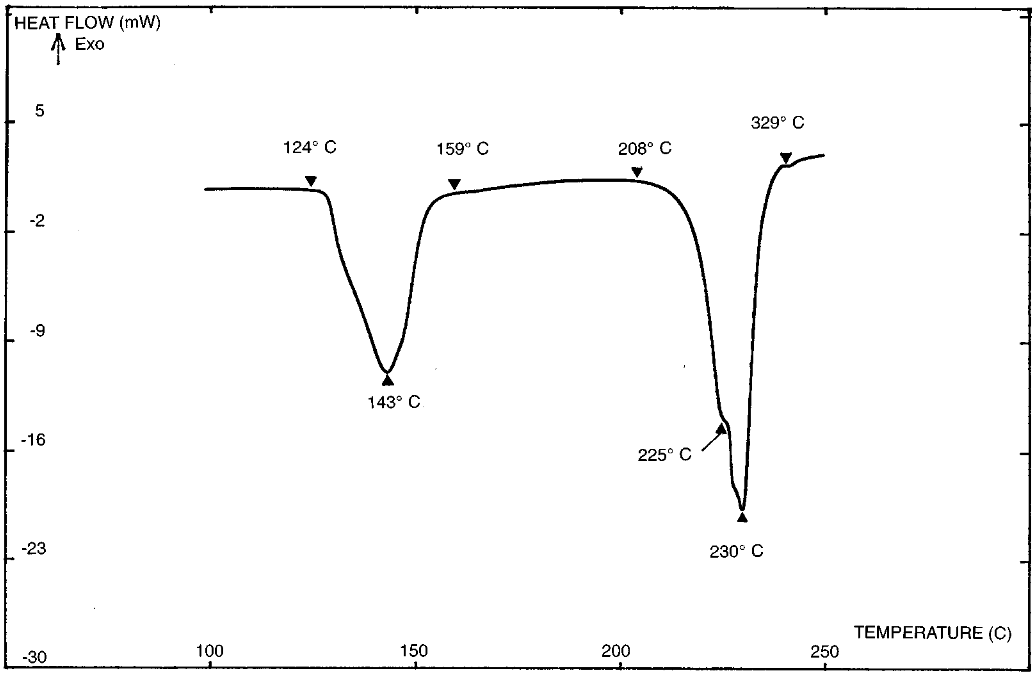

FIG. 6. DSC curve of DAPHP.

the first two regions of the TG–DTA curves. Indeed, the second shouldered endothermic effect corresponds to both evolution of ammonia and melting of the anhydrous compound. This combined effect was recently observed in the organic cyclohexaphosphate $[C_6H_{18}N_3]_2P_6O_{18} \cdot 6H_2O$ (4). The first endothermic peak, occurring in the temperature range 124–159°C (Fig. 6), corresponds to the dehydration with $\Delta H = 42.98$ kJ/mol. The overall ΔH of the elimination of ammonia and fusion, occurring in the region 208–239°C, is 57.72 kJ/mol.

Figure 7 shows both TG and DTA thermograms of TMEDH2P from room temperature to 300°C. The weight loss is divided into three areas, 53–106, 106–176, and 176–210°C, and the total weight loss is found to be 18.86%, close to the calculated value, 18.75%. The TG weight loss (13.82%) in the first two ranges, due to the elimination of three H_2O molecules, is close to the calculated value (14.06%) and related to the first large endotherm and the set of endothermic peaks as shown in the DTA curve. The last water molecule of the structure is evolved in the third temperature area, since the experimental weight loss (5.44%) is close to the calculated value (5.45%). Thus, all endotherms are considered to result from the evolution of the water from the structure. Tested by IR and XRD, the resulting, still white, powder exhibits infrared bands characteristic of the monophosphate anion and a well-crystallized anhydrous compound. The differential calorimetric study, displayed in Fig. 8, shows a large shouldered endotherm in the range 50–80°C, followed by a set of endotherms from 80 to 170°C assigned to the dehydration of three molecules of water, in accordance with the TG–DTA study. The overall ΔH of this dehydration is found to be 115.44 kJ/mol. The endothermic peak at 187°C corresponds to the elimination of the last water molecule from the structure with $\Delta H = 20.47$ kJ/mol. The exotherm at 197°C is probably due to the enhanced partial pressure of water vapor. All endothermic peaks are shifted to a low temperature by a decrease in the run heating from 5°C/min (TG–DTA) to 3°C/min (DSC).

On the other hand, the baselines, as shown in the DTA curves (Figs. 5 and 7), are gently sloping up, and their slopes may change with temperature. Such premonitory phenomena may be associated with an increase of atomic motions—in the sample in particular, the increase of disorder—as the decomposition is approached. This decomposition, with ammonia evolution by the pyrolysis, is confirmed as follows: An effluent dry nitrogen is introduced continuously into $30\,cm^3$ of 0.01 mol/l sulfuric acid at $50\,cm^3$/min. The gas is passed into the acid for a further 30 min after the TG–DTA furnace has reached the required temperature to absorb any ammonia remaining in the sealed device. The ammonia absorbed in the solution is determined by means of a back-titration technique, using a 0.02 mol/l sodium hydroxide solution and a pH meter. Thus, the thermal decomposition of DAPHP and TMDH2P can be described by, first, the elimination of water molecules and then the evolution of ammonia when the temperature of pyrolysis is reached.

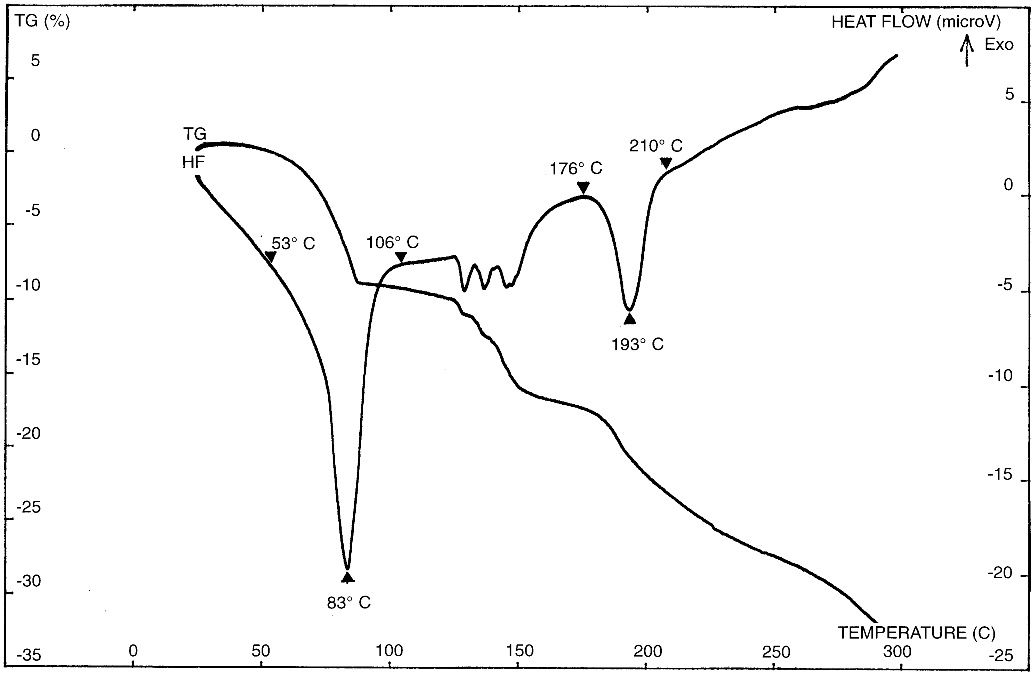

FIG. 7. TG–DTA analysis of TMEDH2P.

V. CONCLUSION

DAPHP and TMEDH2P exhibit two kinds of polyanion organizations, infinite ribbons and chains. Organic cations connect them through two types of hydrogen-bonding networks. Strong hydrogen bonds of type O–H ··· O built the polyanions, which are themselves interconnected with the organic groups through the second type of hydrogen bonds,

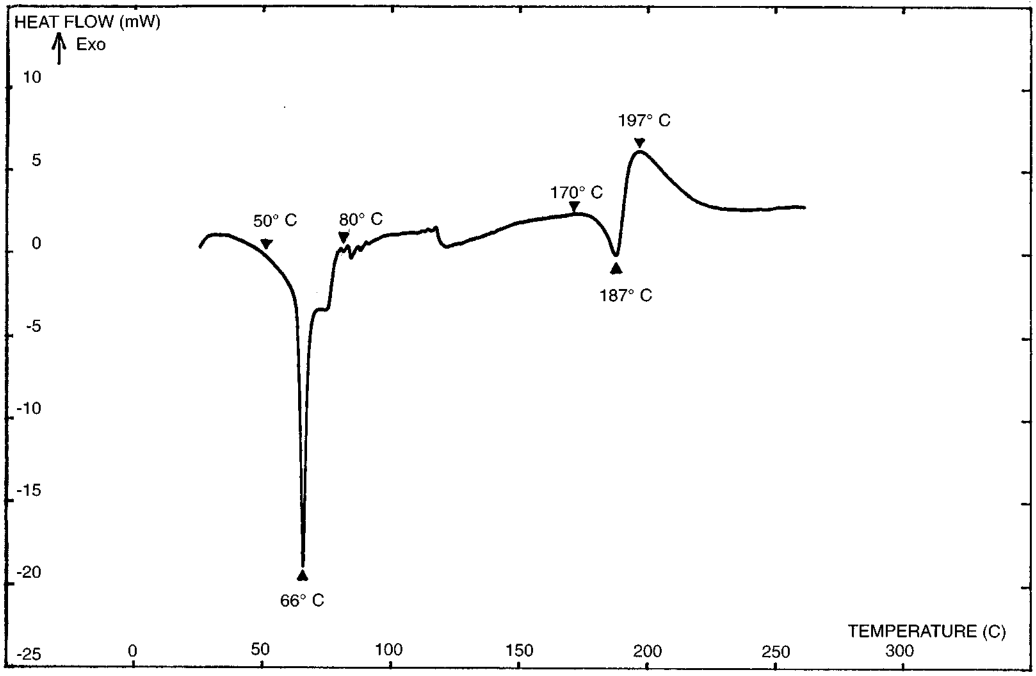

FIG. 8. DSC curve of TMEDH2P.

namely, N–H ⋯ O originating from the N–H donors. The thermal behavior studies, summarized by elimination of the water molecules and the evolution of ammonia when the temperature of pyrolysis is reached, specify the stability of the DAPHP and TMDH2P compounds. The only difference between these two compounds is the melting of DAPHP before pyrolysis whereas the TMEDH2P degrades without melting.

ACKNOWLEDGMENTS

The authors express their most grateful thanks to Dr. T. Jouini, Département de Chimie, Faculté des Sciences de Tunis, Tunisia, for the X-ray data collection.

REFERENCES

1. A. Gharbi, A. Jouini, M. T. Averbuch-Pouchot, and A. Durif, *J. Solid State Chem.* **111,** 330 (1994).
2. H. Thabet and A. Jouini, *Acta Crystallogr., Sect. C* **52,** 2248 (1996).
3. H. Thabet, M. Bdiri, A. Jouini, and A. Durif, *J. Soc. Chim. Tunisie* **3,** 693 (1995).
4. M. Charfi and A. Jouini, *J. Solid State Chem.* **127,** 9 (1996).
5. M. Bagieu-Beucher, R. Masse, and D. Tran Qui, *Z. Anorg. Allg. Chem.* **606,** 59 (1991).
6. S. Kamoun, A. Jouini, and A. Daoud, *Acta Crystallogr., Sect. C* **46,** 1481 (1990).
7. R. Masse and A. Durif, *Z. Kristallogr.* **190,** 19 (1990).
8. J. Zaccaro, M. Bagieu-Beucher, A. Ibanez, and R. Masse, *J. Solid State Chem.* **124,** 8 (1996).
9. G. M. Sheldrick, *Acta Crystallogr. Sect. A* **46,** 467 (1990).
10. G. M. Sheldrick, "SHELXL93: Program for the Refinement of Crystal Structures," University of Göttingen, Germany.
11. Enraf-Nonius, "Structure Determination Package," Enraf-Nonius, 1980.
12. P. Main, S. E. Hull, L. Lessinger, G. Germain, J. P. Declercq, and M. M. Woolfson, "MULTAN77, a System of Computer Programs for the Automatic Solution of Crystal Structures from X-ray Diffraction Data," University of York, England, and Catholic University of Louvain, Belgium, 1977.
13. "International Tables for X-Ray Crystallography," Vol. IV. Kynoch Press, Birmingham, 1974 (distributed by Kluwer Academic Publishers, Dordrecht).
14. M. Bagieu-Beucher, Y. Le Fur, J. P. Levy, and J. Pécaut, *Acta Crystallogr., Sect. C* **50,** 1079 (1994).
15. I. Brown, *Acta Crystallogr., Sect. A* **32,** 24 (1976).
16. R. Taylor and O. Kennard, *J. Chem. Soc.* **104,** 5063 (1982).
17. Th. Steiner and W. Saenger, *J. Chem. Soc.* **115,** 4540 (1993).
18. Th. Steiner and W. Saenger. *Acta Crystallogr., Sect. B* **50,** 348 (1994).
19. G. Ferraris and G. Ivaldi, *Acta Crystallogr., Sect. B* **40,** 1 (1984).
20. A. Gharbi, M. Charfi, and A. Jouini, *Acta Crystallogr., Sect. C* **52,** 2246 (1996).